Electronic structure of superconducting copper intercalated transition metal dichalcogenides: First-principles calculations

R. A. Jishi and H. M. Alyahyaei
Department of Physics, California State University, Los Angeles, California 90032, USA
(Received 12 January 2008; revised manuscript received 14 August 2008; published 27 October 2008)

We report first-principles calculations, within density functional theory, of copper intercalated titanium diselenides, Cu_xTiSe_2, for values of x ranging from 0 to 0.11. The effect of intercalation on the energy bands and density of states of the host material is studied in order to better understand the cause of the superconductivity that was recently observed in these structures. We find that charge transfer from the copper atoms to the metal dichalcogenide host layers leads to the formation of Cu-Se bonds that stabilize most of the transferred charge on Se atoms and lead to a relatively large lowering of the Se-derived hole bands. The suppression of the hole bands, the increase in the number of electrons, and the corresponding enhancement of the density of states at the Fermi energy may contribute to the emergence of superconductivity in these systems.

DOI: 10.1103/PhysRevB.78.144516 PACS number(s): 74.70.Dd, 71.45.Lr, 71.20.Be

I. INTRODUCTION

Transition metal dichalcogenides (TMDCs) are quasi-two-dimensional, highly anisotropic layered compounds that are of great interest in basic research, as well as in applications in areas such as lubrication, catalysis, electrochemical photocells, and battery systems.[1] Recently, it became possible to synthesize other forms of TMDCs such as balls and nanotubes.[2–4] TMDCs generally have the formula MX_2, where M is a transition metal such as vanadium, titanium, tantalum, molybdenum, or others, and X is a chalcogen atom such as sulfur, selenium, or tellurium. Each layer consists of a metal sheet sandwiched between two chalcogen sheets. Whereas within each layer the bonds connecting a metal atom in one sheet to the chalcogen atoms in surrounding sheets are strong partially ionic and partially covalent bonds, adjacent layers are only weakly coupled through the van der Waals interaction. Two types of MX_2 sandwiches occur depending on the coordination of the transition metal atom by the chalcogens. In 1T-MX_2 the coordination is octahedral, whereas in 2H-MX_2 it is trigonal prismatic.

The weak coupling between adjacent layers in TMDCs makes it possible to introduce foreign species into the region between these layers, a region called the van der Waals gap. This process, known as intercalation, provides the ability to tune the electronic properties of the system by controlling the type and concentration of the intercalant. This is a general property of layered materials, and just like graphite, which has been intercalated with many kinds of atoms and molecules,[5] TMDCs have been intercalated with alkali atoms, transition metal atoms, and organic and inorganic molecules.[1]

Among the most important properties of TMDCs is that some of them undergo a phase transition to a charge-density wave (CDW) state as the temperature is lowered.[6] 1T-$TiSe_2$ is one of the first compounds where the CDW state was observed at temperatures below 200 K.[6–8] The state is associated with the formation of a commensurate $(2\times2\times2)$ superlattice. It is not completely clear what mechanism drives this phase transition. Possible explanations are offered in terms of an indirect Jahn-Teller effect[9,10] or by an exciton condensation mechanism.[11,12]

Recent angle-resolved photoemission spectroscopy (ARPES) studies have not resolved whether 1T-$TiSe_2$ is a semimetal with low electron and hole concentration or a narrow-gap semiconductor in either the normal or the CDW state.[13–15] Optical measurements, on the other hand, reveal that $TiSe_2$ is a semimetal with low carrier density at temperatures above as well as below the CDW transition.[16] This is consistent with band-structure calculations,[17] which reveal the presence of an electron pocket around the L point in the Brillouin zone (BZ), derived from Ti $3d$ states and a hole pocket around the Γ point derived from Se $4p$ states.

Recently it was reported[18] that upon controlled intercalation of $TiSe_2$ with Cu to yield Cu_xTiSe_2, the CDW transition is continually suppressed, making way for a superconducting state that emerges near $x=0.04$ with a maximum transition temperature T_c of 4.15 K occurring at $x=0.08$; further increase in x results in a drop in T_c. It should be noted that while superconductivity was previously observed in 2H structures, such as 2H-$NbSe_2$, 2H-$TaSe_2$, 2H-NbS_2, and 2H-TaS_2,[19] the copper intercalated $TiSe_2$ is the first superconducting 1T-structured TMDC. As Cu atoms are intercalated, they move into the van der Waals gap separating adjacent $TiSe_2$ layers. With a single electron in the outer $4s$ shell, electronic charge transfer proceeds from Cu to the $TiSe_2$ layers, causing an increase in the number of electrons in the Ti $3d$ bands and a reduction in the number of holes in the Se $4p$ bands. It is observed that for a copper concentration $x=0.06$ the CDW transition is completely suppressed. The superconducting transition, on the other hand, emerges at $x=0.04$. Recently, calculations of density of states (DOS) and the electron-phonon coupling, using linear muffin-tin orbital (LMTO) method within the local density approximation (LDA), were reported for the case $x=0.08$ by Jeong and Jarlborg.[20] The authors considered a $2\times2\times3$ supercell, $Cu(TiSe_2)_{12}$, and concluded that charge transfer from copper raises the electronic density of states at the Fermi energy. They also find a strong dependence on pressure of the DOS and consequently the superconducting transition temperature.

In this work we calculate the energy bands of copper intercalated $TiSe_2$ for different values of copper concentration

and compare them with those of undoped $TiSe_2$. We show that the addition of copper has a strong influence on the Se-derived bands. By studying the distribution of charge transferred from the copper intercalant to the host layers, we argue that bonds are formed between a copper atom and neighboring Se atoms. Those bonds stabilize the transferred charge on the Se atoms and lower the energy of the Se-derived bands. We also calculate the density of states at the Fermi level and show that it is enhanced by copper intercalation, in agreement with the calculations of Jeong and Jarlborg.[20] In Sec. II we discuss the computational method and some relevant details, in Sec. III we discuss the results, and in Sec. IV conclusions are presented.

II. METHOD

The first-principles calculations presented in this work were performed using the all-electron full potential linear augmented plane wave plus local orbitals (FP-LAPW+lo) method as implemented in WIEN2K code.[21] In this method the core states are treated in a fully relativistic way, but the valence states are treated at a scalar relativistic level. The exchange-correlation potential was calculated using the generalized gradient approximation (GGA) as proposed by Pedrew, Burke, and Ernzerhof (PBE).[22]

In the calculations on 1T-$TiSe_2$ the experimentally measured lattice constants ($a=b=3.534$ Å, $c=6.008$ Å) are employed.[23] The distance between the Ti plane and either of the adjacent Se planes is $d=zc$, where the value of z is obtained by minimizing the forces on the atoms to below 2.0 mRy/Bohr. In calculations on the intercalated compounds $Cu(TiSe_2)_n$ the lattice constants are taken to coincide with the experimental values,[18] but the internal structure of the unit cell is allowed to relax, subject only to the constraint that the space group remains unchanged; again the force on each atom is reduced to below 2.0 mRy/Bohr. For the compound $Cu(TiSe_2)_{16}$ the structure is taken to be that of $TiSe_2$ 4×4 superlattice in the a-b plane with one Cu atom placed midway between one Ti atom in one layer and the nearest Ti atom in the adjacent layer; the unit cell is then hexagonal with $a'=b'=4a$. Accordingly, the unit cell has one Cu atom, 16 Ti atoms, and 32 Se atoms, and if one Ti atom is placed at the origin (0,0,0), then the Cu atom is placed at $(0,0,c'/2)$, where c' is the lattice parameter, in the direction normal to the a-b plane, in the intercalated systems. A similar situation holds for $Cu(TiSe_2)_9$ and $Cu(TiSe_2)_{13}$, where the corresponding superlattices in the a-b plane are 3×3 and $\sqrt{13}\times\sqrt{13}$, respectively. The space group is P-3m1(164), the same as in $TiSe_2$, in all these structures, except in $Cu(TiSe_2)_{13}$, where it is P-3(147). It should be noted here that the superlattice structure employed in these calculations is not necessarily the experimental lattice structure. For example, for the case $x=0.0625$, we assume that the system is periodic with lattice constants in the a and b directions that are four times bigger than the corresponding values for $x=0$, whereas the experimental crystal structure is not reported and there may well be some disorder in the system such that the Cu atoms, residing between adjacent TMDC layers, do not form a perfectly periodic two-dimensional lattice.

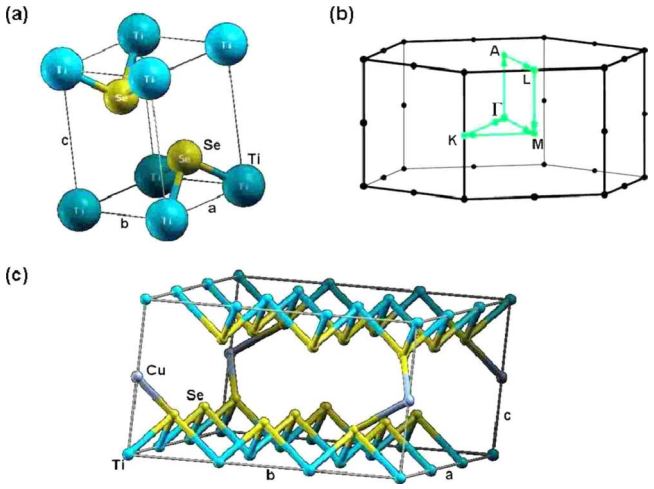

FIG. 1. (Color online) The unit cell of $TiSe_2$ is shown in (a), while the Brillouin zone and the k path along which the energy bands are calculated are shown in (b). In (c), the unit cell for $Cu(TiSe_2)_9$ is shown.

For calculations in this work, the radii of the muffin-tin spheres for Cu, Ti, and Se atoms were taken to be $2.5a_0$, $2.5a_0$, and $2.25a_0$, respectively, where a_0 is the Bohr radius. The number of k points in the irreducible part of the BZ were 38, 41, 47, and 360 for $Cu(TiSe_2)_{16}$, $Cu(TiSe_2)_{13}$, $Cu(TiSe_2)_9$, and $TiSe_2$, respectively; these numbers were chosen so that the density of k points in the whole BZ is roughly the same in the four cases. For all structures considered in this work we set the parameter $R_{MT}K_{max}=7$, where R_{MT} is the smallest muffin-tin radius and K_{max} is a cutoff wave vector. The valence wave functions inside the muffin-tin spheres are expanded in terms of spherical harmonics up to $l_{max}=10$, while in the interstitial region they are expanded in plane waves with a wave-vector cutoff K_{max}, and the charge density is Fourier expanded up to $G_{max}=14a_0^{-1}$. Convergence of the self-consistent field calculations is attained with a total energy convergence tolerance of 0.1 mRy.

III. RESULTS AND DISCUSSION

It is well known that the calculation method followed in this work (GGA and PBE) overestimates the unit-cell volume and lattice constants, and it gives a very large c/a value in layered compounds.[24,25] Indeed, upon optimization, Titov *et al.*[26] obtained a value for c/a in $TiSe_2$, which is about 5% larger than the experimental value. Since the lattice constants are known for $TiSe_2$ and its copper intercalated compounds, we perform the calculations using these experimental values, but we allow the internal coordinates to relax.

The unit cell of $TiSe_2$, shown in Fig. 1(a), consists of one Ti atom and two Se atoms. The crystal coordinates of these atoms are given by Ti(0, 0, 0), Se1(1/3, 2/3, z), and Se2(2/3, 1/3, $-z$). Upon minimizing the forces on each atom to below 2 mRy/Bohr, it is found that $z=0.2573$; the distance between the Ti plane and an adjacent Se plane is thus 1.546 Å. The BZ corresponding to the $TiSe_2$ structure is shown in Fig. 1(b), and the calculated energy bands along some high-

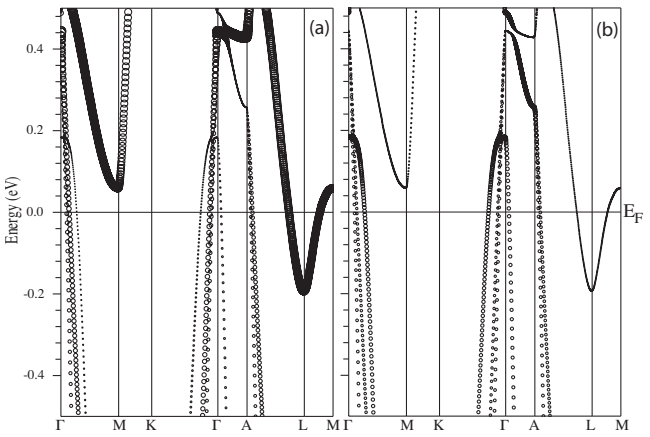

FIG. 2. Band character plot for $TiSe_2$ along high-symmetry directions in the Brillouin zone (BZ). In (a), the contribution from Ti 3*d* states is shown. The width of the band lines is proportional to the contribution of the Ti 3*d* states to these bands. In a band character plot, every point is replaced by a circle whose radius is proportional to the contribution of the emphasized state to the Bloch wave function at the corresponding *k* point in the BZ. In (b), the contribution of the Se 4*p* states to the energy bands is emphasized. The Fermi level is at zero energy.

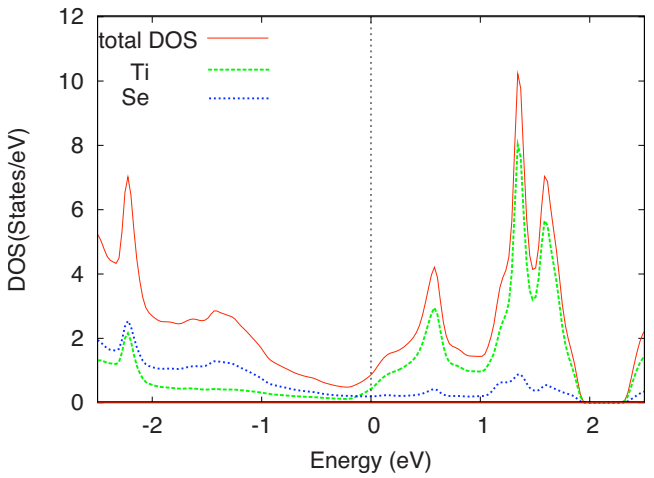

FIG. 3. (Color online) Total and atomic densities of states in $TiSe_2$. More than half of the total DOS at the Fermi energy is due to the Ti states.

symmetry directions in the BZ are shown in Fig. 2. In Fig. 2(a) the contribution to the bands from the Ti 3*d* states is shown, while in Fig. 2(b) the contribution from the Se 4*p* states is displayed. The bands are in broad agreement with previous calculations.[17] However, they are only in qualitative agreement with a recent ARPES study,[27] which shows that 1T-$TiSe_2$ has a semimetallic band structure with a negative energy gap $E_G = -70 \pm 15$ meV, the Se 4*p* band having a maximum at 30 ± 10 meV and the Ti 3*d* band having a minimum at -40 ± 5 meV with respect to the Fermi energy. The agreement is only qualitative in the sense that our calculations show that $TiSe_2$ is semimetallic with a negative energy gap. Calculations using methods such as LDA or GGA are known to fail in producing the correct size of the energy gap, and a more accurate treatment of correlations is needed to obtain quantitative agreement with the experimental values of energy gaps.[25] By examining these plots, it is observed that the electron pocket at *L*, with a minimum at ~ -0.18 eV, is derived mainly from Ti 3*d* states, while the hole pockets at Γ and *A* are derived from Se 4*p* states with some significant hybridization with the Ti 3*d* states. In particular, the hole band with a maximum at the Γ point at ~ 0.17 eV is derived from Se 4*p* states, while the other two hole bands with a maximum at ~ 0.4 eV at the Γ point result from hybridization between the Ti 3*d* and Se 4*p* states.

The calculated density of states (DOS) in $TiSe_2$ is plotted in Fig. 3 along with the partial densities of Ti-derived and Se-derived states. It is noted that at the Fermi level, more than half the total DOS results from Ti states and that the DOS of Se states is about half that of the Ti states; the rest of the DOS results from the interstitial region between the muffin-tin spheres. Note that for negative energies, well below the Fermi energy, the Ti and Se atomic densities of states have similar variation with energy. This is a reflection of the strong bonding between the Ti and Se atoms.

Upon intercalation by copper, the *c* axis is increased slightly, and some slight rearrangement of the positions of the Se atoms takes place. The new positions are found by relaxing the structure so as to minimize the forces acting on the atoms. The lattice constants are held fixed at the experimental values, while the internal coordinates are allowed to change. We find that the incorporation of copper atoms between $TiSe_2$ layers leads to only a slight modification in the atomic positions. To illustrate this point, we present in Table I the coordinates of the inequivalent atoms for the case of $Cu(TiSe_2)_9$ in the ideal superlattice structure (before optimization) and the corresponding coordinates after optimization. In the three compounds, $Cu(TiSe_2)_n$, for $n=16$, 13, and 9, the Se atoms are displaced in the *z* direction by δz, where -0.006 Å $< \delta z < 0.009$ Å, whereas they are displaced in the *a*-*b* plane by less than 0.037 Å. Because of the slight displacement in the *z* direction of the Se atoms, they no longer all lie in a single plane as is the case in undoped $TiSe_2$. Nevertheless, our results indicate that the disturbance caused by intercalating copper into the van der Waals gaps of $TiSe_2$ is small as far as its effect on the atomic positions is concerned. This is not unusual; a similar situation holds in graphite intercalation compounds, where, besides an increase in the *c* lattice constant, the effect on the structure of the carbon planes is minimal. This is a consequence of the fact that both in $TiSe_2$ and graphite, the bonding within each layer (in $TiSe_2$ a layer consists of three atomic sheets) is strong.

The intercalation of copper into the van der Waals gap in $TiSe_2$ is stabilized by charge transfer from copper to the TMDC layers. Here we calculate the charge on each atom using Bader's quantum theory of "atoms in molecules" (AIM).[28] In this theory space is divided among the atoms so that each atom occupies a definite volume bounded by a surface at which the flux in the gradient of the electron density $\rho(\vec{r})$ vanishes,

TABLE I. Comparison of the crystal structure of $Cu(TiSe_2)_9$ before optimization, as derived from the structure of $TiSe_2$, with the relaxed structure obtained by minimizing the forces on the atoms. The space group of the crystal is P-3m1.

		a/Å 10.641			c/Å 6.044		
		Ideal superlattice (before optimization)			After optimization		
Atom	Site	x	y	z	x	y	z
Ti(1)	1a	0	0	0	0	0	0
Ti(2)	6g	1/3	0	0	0.3362	0	0
Ti(3)	2d	2/3	1/3	0	2/3	1/3	0.000455
Se(1)	6i	1/9	2/9	0.2573	0.1134	0.2267	0.2561
Se(2)	6i	4/9	2/9	0.2573	0.4447	0.2224	0.2548
Se(3)	6i	4/9	8/9	0.2573	0.4446	0.8891	0.2572
Cu	1b	0	0	1/2	0	0	1/2

$$\hat{n}(\vec{r}) \cdot \vec{\nabla}\rho(\vec{r}) = 0,$$

where $\hat{n}(\vec{r})$ is a unit vector normal to this bounding surface at $\vec{r}$. The number of electrons in a given atom, occupying a volume Ω, is then given by

$$N_e = \int_{\Omega} \rho(\vec{r}) d^3 r.$$

For undoped $TiSe_2$ we find that Ti is positively charged with a charge of $1.575e$, while each Se has a negative charge of $-0.787e$. In the intercalated compounds $Cu(TiSe_2)_n$ we find that the copper atom acquires a positive charge of $0.445e$, $0.444e$, and $0.450e$ for $n=9$, 13, and 16, respectively. To illustrate how the charge is distributed we present in Table II the charge on each atom in the case of $Cu(TiSe_2)_9$, as calculated by Bader's AIM theory.

For the copper intercalated systems, the energy bands appear to be far more complicated than in undoped $TiSe_2$ because the unit cell has many more atoms. A direct comparison between the undoped $TiSe_2$ energy bands and those of the doped compounds is not very helpful in clearly elucidating the effect of copper intercalation. Most of the bands in the intercalated compounds result from the zone folding, into the smaller BZ, of the bands in the larger BZ of the pristine compound. Therefore, in order to gauge accurately the effect of intercalation with copper on the energy bands, it is more useful to compare the bands in the Cu intercalated $TiSe_2$ with those that result from zone folding the pristine $TiSe_2$ bands into the smaller BZ characteristic of the intercalated compounds. For example, the compound $Cu(TiSe_2)_{16}$, except for a slight variation in the c lattice parameter and an extra Cu atom, has a unit cell which is the same as that of a $4\times4\times1$ superlattice of pristine $TiSe_2$, which also consists of 16 $TiSe_2$ units. To understand the effect of the addition of copper in this case, we compare the energy bands of $Cu(TiSe_2)_{16}$ with those of $(TiSe_2)_{16}$, the $4\times4\times1$ undoped $TiSe_2$ superlattice. Similar arguments apply in the case of intercalation compounds for other values of the copper concentration.

TABLE II. The charge on each inequivalent site in $Cu(TiSe_2)_9$, as calculated by AIM theory, and the corresponding change in the charge on each site resulting from copper intercalation. Note that the charge of an electron is $-e$ so that e is positive.

Atom	Site	Q/e	$\Delta Q/e$
Ti(1)	1a	1.551	−0.024
Ti(2)	6g	1.563	−0.012
Ti(3)	2d	1.577	+0.002
Se(1)	6i	−0.820	−0.033
Se(2)	6i	−0.801	−0.014
Se(3)	6i	−0.796	−0.009
Cu	1b	0.445	+0.445

The energy bands of the systems studied in this work are shown in Figs. 4–6. In Fig. 4 we compare the energy bands of the $4\times4\times1$ superlattice with those of $Cu(TiSe_2)_{16}$. It should be noted that for the $4\times4\times1$ superlattice, the BZ is 16 times smaller than that for pristine $TiSe_2$. The M and L

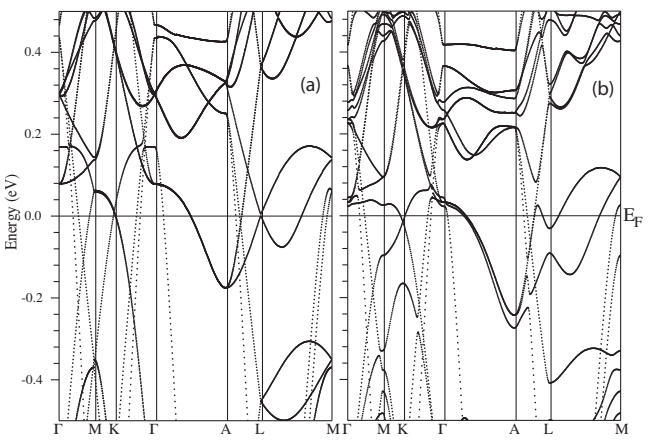

FIG. 4. Energy bands for the $4\times4\times1$ $TiSe_2$ superlattice are shown in (a), while those for $Cu(TiSe_2)_{16}$ are shown in (b). The Fermi level is at zero energy.

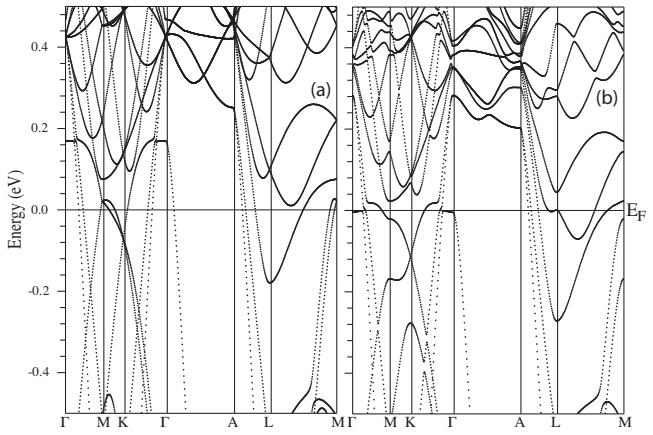

FIG. 5. Energy bands for the $\sqrt{13}\times\sqrt{13}\times 1$ $TiSe_2$ superlattice obtained by zone folding of the $TiSe_2$ bands and the energy bands for $Cu(TiSe_2)_{13}$ are shown in (a) and (b), respectively. The Fermi level is at zero energy. Note that while the Fermi level rises by only 0.06 eV, as a result of Cu intercalation, the hole band—with a maximum at 0.17 eV at Γ in (a)—shifts down in energy to just below Fermi level.

points in the pristine $TiSe_2$ BZ are zone folded into the Γ and A points, respectively, in the superlattice BZ; this explains why features in the band structure at the M and L points in Fig. 2 now appear at points Γ and A, respectively, in Fig. 4. For example, in Fig. 4(a), the band along ΓA, which crosses the Fermi level, and which is derived from Ti 3*d* states, corresponds to the band along ML in the pristine $TiSe_2$ BZ; the M point is folded to Γ and the L point is folded to A. On the other hand the M and L points in the pristine $TiSe_2$ BZ are zone folded into the M and L points, respectively, in $3\times 3\times 1$ or $\sqrt{13}\times\sqrt{13}\times 1$ superlattice BZ.

By closely examining the energy bands of the pristine and copper intercalated $TiSe_2$ compounds, we observe that although the addition of Cu leads only to a slight rise in the

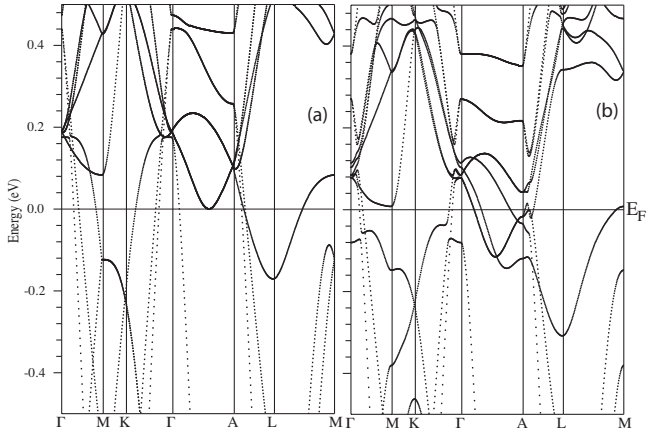

FIG. 6. Energy bands for the $3\times 3\times 1$ $TiSe_2$ superlattice, obtained by zone folding of the $TiSe_2$ bands, are shown in (a), while the bands of the copper intercalated compound $Cu(TiSe_2)_9$ are shown in (b). The Fermi level is at zero energy. Note the rise by 0.08 eV of the Fermi level in (b) as compared to (a). The hole band, with a maximum at 0.17 eV at Γ in (a), shifts down in energy to −0.08 eV as a result of copper intercalation. A similar fate meets the hole band at A.

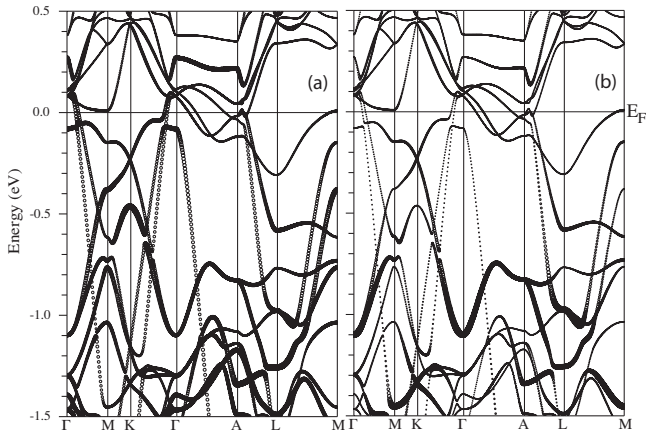

FIG. 7. Band character plot for $Cu(TiSe_2)_9$ along high-symmetry directions in the Brillouin zone. In (a) the Se(1) 4p character is emphasized while in (b) the Cu 3*d* character is displayed. For energies well below the Fermi energy there are bands with mixed Se 4*p* and Cu 3*d* character, reflecting the significant hybridization between Se and Cu states.

Fermi energy level, the lowering in energy of the Se-derived hole bands far exceeds this rise in the Fermi level. For example, the energy bands plot for $Cu(TiSe_2)_9$, shown in Fig. 6, shows that while the Fermi level is raised by ~0.08 eV due to copper intercalation, the hole pockets at Γ and A are lowered by ~0.25 eV. How do we understand this? By examining the density of states plot in $TiSe_2$, shown in Fig. 3, we note that in a rigid band model it is expected that more than half the charge transferred from Cu should occupy Ti-derived states. In other words, if we simply add electrons to $TiSe_2$, along with a compensating positive background, more of the added electrons will reside on the Ti atoms rather than the Se atoms because of the larger DOS, at the Fermi level, of the Ti-derived states. Yet the distribution of the transferred charge, as obtained earlier from AIM analysis, indicates otherwise; 80% of the charge transferred from Cu resides on Se atoms. This suggests that the rigid band model fails in describing the effect of copper intercalation on the electronic structure of $TiSe_2$, and it points to an active role played by the copper ions in stabilizing the transferred charge on Se atoms through the formation of Cu-Se bonds. This conclusion is made plausible by the following two observations:

(i) The separation between the Cu ion and the nearest Se ions is only slightly larger than the Cu-Se bond length in crystals containing Cu and Se. For example, in $Cu(TiSe_2)_9$ the Cu-Se(1) separation is 2.557 Å, while the Cu-Se bond length is 2.44 Å in Cu_2Se (Ref. 29) and 2.4337 Å in $CuInSe_2$.[30]

(ii) Significant hybridization takes place between the Cu and Se states; this is revealed by the band character plots in Fig. 7. This hybridization results in bonding states with a mixed character; indeed for energies below −0.5 eV, several bands have contributions from both Cu 3*d* states and Se(1) 4*p* states. This indicates that the Cu atoms are not simply passive electron donors, but that they stabilize the transferred charge on the Se atoms.

The nature of the Cu-Se(1) bond is elucidated by examining the electron density plot shown in Fig. 8 for

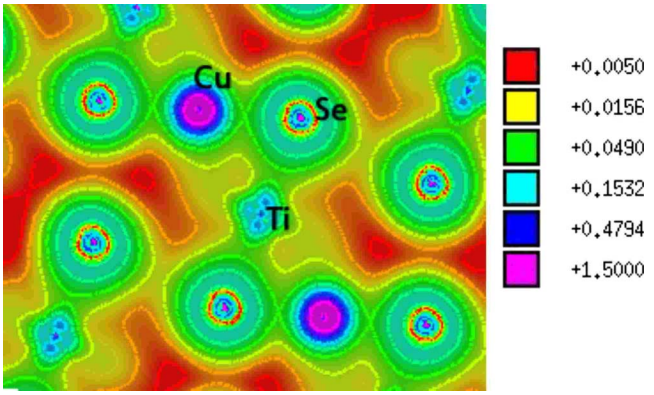

FIG. 8. (Color online) Electron density plot (in e/a_0^3) for $Cu(TiSe_2)_9$. The density is plotted in a plane formed by Cu, Se(1), and Ti(1) atoms. Along a contour the electron density is constant.

$Cu(TiSe_2)_9$. Here, the electron density is plotted in a plane formed by Cu, Se(1), and Ti(1) atoms; the plot shows that the Cu-Se(1) bond is partially ionic and partially covalent.

Now we offer some comments on a possible explanation for the suppression of the CDW state in $TiSe_2$ upon copper intercalation. The exciton condensation model was proposed as a possible explanation for the emergence at low temperature of a CDW state in a semimetal or a narrow-gap semiconductor.[11,12] If in the BZ there is an electron pocket and a hole pocket, separated by a certain wave vector, then the Coulomb attraction between an electron and a hole leads to the formation of a bound state known as an exciton. The exciton binding energy depends on the strength of the Coulomb interaction, which, for sufficiently small number of carriers, is only weakly screened. As the number of the excitons increases, and being composite bosons, they condense into one state with an electronic density displaying a periodicity different than that of the original lattice. In some cases, this is accompanied by a lattice distortion. Recently, some evidence was provided by Cercellier *et al.*[27] to indicate that the CDW state in $TiSe_2$ results from such a mechanism, with excitons being formed from electrons in the pocket at the L point in the BZ and holes in the pocket at the Γ point. Our calculations show that as the copper concentration increases, the number of electrons in the electron pocket increases while the number of holes is reduced. This causes a reduction in the number of excitons. Furthermore, the electron-hole Coulomb interaction is now more strongly screened due to the increase in the number of electrons and the resulting enhancement of the density of states at the Fermi energy. A small amount of thermal energy may then be sufficient to separate the exciton into a free electron and a free hole. Thus, our calculations, though they do not provide any proof as to the nature of the CDW state in $TiSe_2$, or the driving mechanism behind this low-temperature phase, yet they are consistent with the experimentally observed suppression of the CDW state, as the copper concentration increases,[18] if exciton condensation is assumed to be the mechanism behind the transition to the CDW state.

The emergence of superconductivity, as the concentration of Cu increases, is probably related to the suppression of the CDW transition and the concomitant increase in the electronic density of states in the vicinity of the Fermi level. We calculated the density of states for the various systems considered in this work, and in Table III we present the calculated density of states at the Fermi energy, in states per eV per one $TiSe_2$ unit, for pristine $TiSe_2$, as well as the other various intercalation compounds. According to the BCS theory of superconductivity,[31] the transition temperature T_c increases with an increase in the density of states in the immediate vicinity of the Fermi level, the other important factor affecting T_c being the strength of the electron-phonon coupling. It is noted that intercalation by Cu causes an enhancement of the DOS at the Fermi energy; this is consistent with the emergence of superconductivity in the intercalated systems. It should be remarked that the density of states at the Fermi energy, $N(E_F)$, is not necessarily an increasing function of x, the copper concentration, as Table III clearly indicates. The value of $N(E_F)$ is intimately connected to the band structure. As x increases, the Fermi level rises; consequently, the number of bands crossing the Fermi level may change, or that a band will cross the Fermi level at a new k point in the BZ, where DOS may have a larger or a smaller value than at the old k point. For example, in $Cu(TiSe_2)_{13}$, the band structure plotted in Fig. 5 indicates that there are bands that are almost dispersionless in a small region of the BZ around the Γ and L points. Such bands with small dispersion make a large contribution to the DOS. To relate fully the DOS values to the energy band structure, however, one should consider the bands throughout the irreducible part of

TABLE III. The calculated electronic density of states at the Fermi level $N(E_F)$, in states per eV per one $TiSe_2$ unit, for $TiSe_2$ and its copper intercalation compounds.

Compound	$N(E_F)$
$TiSe_2$	0.86
$Cu(TiSe_2)_{16}$	1.06
$Cu(TiSe_2)_{13}$	1.22
$Cu(TiSe_2)_9$	1.01

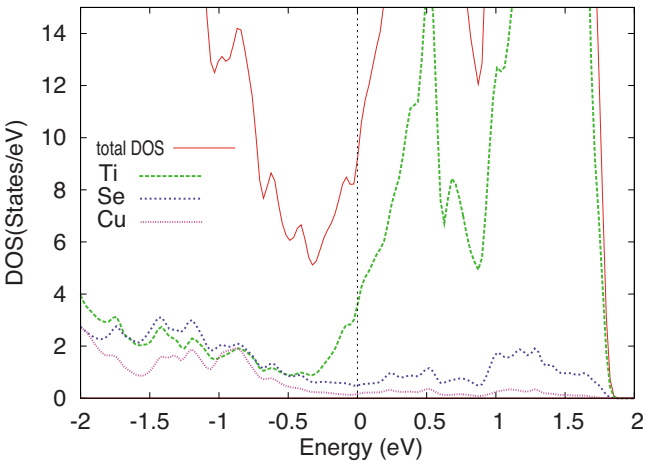

FIG. 9. (Color online) Total and atomic densities of states for $Cu(TiSe_2)_9$. The atomic DOS are shown for three out of the seven inequivalent atoms.

the BZ, not only along high-symmetry directions, since the DOS depends on how the energy of the Bloch electron varies with the wave vector $\vec{k}$ throughout the BZ. As in the case of pristine $TiSe_2$, the DOS of Cu intercalated $TiSe_2$, in the vicinity of the Fermi energy, is also dominated by Ti-derived states. In Fig. 9 we plot the calculated total DOS, along with the atomic DOS of Ti(2), Se(1), and Cu, for the intercalated compound $Cu(TiSe_2)_9$. Note that for energies below ~ -0.5 eV, the three atomic densities of states vary with energy in a similar way, the curves being almost parallel. This is indicative of the strong hybridization between Ti and Se on one hand, as in the case of pristine $TiSe_2$, and between Cu and Se on the other hand. Again, this points to the formation of bonds between the Cu and Se(1) atoms, as discussed earlier. We note that the total DOS is equal to the sum of the atomic DOS and the DOS in the interstitial region. In Fig. 9 we show the total DOS and the atomic DOS for only three out of the seven inequivalent atoms in $Cu(TiSe_2)_9$.

IV. CONCLUSIONS

In conclusion, we have presented calculations, within the density functional theory, of the electronic energy bands and the density of states of copper intercalated $TiSe_2$. The charge transferred from Cu to the host layers is stabilized on the Se atoms by the formation of bonds between the Cu atoms and the neighboring Se atoms. As a result, a relatively large lowering of the energies of the Se-derived states takes place, causing a reduction in the number of holes. Within the exciton condensation model for the transition to the CDW state in $TiSe_2$, this reduction in the number of holes, upon Cu intercalation, suppresses the CDW. Our calculations also show that the electronic density of states in $TiSe_2$, which is one of the factors that affects the superconducting transition temperature, is enhanced upon intercalation by copper.

[1] R. H. Friend and A. D. Yoffe, Adv. Phys. **36**, 1 (1987).
[2] R. Tenne and L. Margolis, Nature (London) **360**, 444 (1992).
[3] G. L. Frey, S. Elani, M. Homyonfer, Y. Feldman, and R. Tenne, Phys. Rev. B **57**, 6666 (1998).
[4] M. Remskar, A. Mrzel, Z. Skraba, A. Jesih, M. Ceh, J. Demsar, P. Stadelmann, F. Levy, and D. Mihailovic, Science **292**, 479 (2001).
[5] M. S. Dresselhaus and G. Dresselhaus, Adv. Phys. **30**, 139 (1981).
[6] J. A. Wilson, F. J. Di Salvo, and S. Mahajan, Adv. Phys. **24**, 117 (1975).
[7] J. A. Wilson and A. D. Yoffe, Adv. Phys. **18**, 193 (1969).
[8] F. J. Di Salvo, D. E. Moncton, and J. V. Waszezak, Phys. Rev. B **14**, 4321 (1976).
[9] T. E. Kidd, T. Miller, M. Y. Chou, and T.-C. Chiang, Phys. Rev. Lett. **88**, 226402 (2002).
[10] C. S. Snow, J. F. Karpus, S. L. Cooper, T. E. Kidd, and T.-C. Chiang, Phys. Rev. Lett. **91**, 136402 (2003).
[11] W. Kohn, Phys. Rev. Lett. **19**, 439 (1967).
[12] B. I. Halperin and T. M. Rice, Rev. Mod. Phys. **40**, 755 (1968).
[13] J. F. Zhao *et al.*, Phys. Rev. Lett. **99**, 146401 (2007).
[14] S. Negishi *et al.*, Physica B **383**, 155 (2006).
[15] X. Y. Cui *et al.*, Phys. Rev. B **73**, 085111 (2006).
[16] G. Li, W. Z. Hu, D. Qian, D. Hsieh, M. Z. Hasan, E. Morosan, R. J. Cava, and N. L. Wang, Phys. Rev. Lett. **99**, 027404 (2007).
[17] A. Zunger and A. J. Freeman, Phys. Rev. B **17**, 1839 (1978).
[18] E. Morosan, H. W. Zandbergen, B. S. Dennis, J. W. G. Bos, Y. Onose, T. Klimczuk, A. P. Ramirez, N. P. Ong, and R. J. Cava, Nat. Phys. **2**, 544 (2006).
[19] A. H. Castro Neto, Phys. Rev. Lett. **86**, 4382 (2001).
[20] T. Jeong and T. Jarlborg, Phys. Rev. B **76**, 153103 (2007).
[21] P. Blaha, K. Schwarz, G. K. H. Madsen, D. Kavasnicka, and J. Luitz, *WIEN2K, an Augmented Plane Wave Plus Local Orbitals Prgram for Calculating Crystal Properties* (Technische Universität, Wien, Austria, 2001).
[22] J. P. Perdew, K. Burke, and M. Ernzerhof, Phys. Rev. Lett. **77**, 3865 (1996).
[23] C. Riekel, J. Solid State Chem. **17**, 389 (1976).
[24] Z. Wu, R. E. Cohen, and D. J. Singh, Phys. Rev. B **70**, 104112 (2004).
[25] D. I. Bilc, R. Orlando, R. Shaltaf, G.-M. Rignanese, J. Iniguez, and Ph. Ghosez, Phys. Rev. B **77**, 165107 (2008).
[26] A. N. Titov, A. V. Kuranov, V. G. Pleschev, Y. M. Yarmoshenko, M. V. Yablonskikh, A. V. Postnikov, S. Plogmann, M. Neumann, A. V. Ezhov, and E. Z. Kurmaev, Phys. Rev. B **63**, 035106 (2001).
[27] H. Cercellier *et al.*, Phys. Rev. Lett. **99**, 146403 (2007).
[28] R. F. W. Bader, *Atoms in Molecules: A Quantum Theory* (Oxford University Press, Oxford, 1990).
[29] A. S. Antsyshkina, G. G. Sadikov, T. I. Koneshova, and V. S. Sergienko, Inorg. Mater. **40**, 1259 (2004).
[30] K. S. Knight, Mater. Res. Bull. **27**, 161 (1992).
[31] J. Bardeen, L. N. Cooper, and J. R. Schrieffer, Phys. Rev. **108**, 1175 (1957).